O-linked glycosylation of von Willebrand factor modulates the interaction with platelet receptor glycoprotein Ib under static and shear stress conditions

Agata A. Nowak,[1] Kevin Canis,[2] Anne Riddell,[3] Michael A. Laffan,[1] and Thomas A. J. McKinnon[1]

[1]Department of Haematology, Faculty of Medicine, Hammersmith Hospital Campus, and [2]Division of Molecular Biosciences, Faculty of Natural Sciences, Imperial College London, London, United Kingdom; and [3]Katharine Dormandy Haemophilia Centre and Thrombosis Unit, The Royal Free and University College Medical School, London, United Kingdom

We have examined the effect of the *O*-linked glycan (OLG) structures of VWF on its interaction with the platelet receptor glycoprotein Ibα. The 10 OLGs were mutated individually and as clusters (Clus) on either and both sides of the A1 domain: Clus1 (N-terminal side), Clus2 (C-terminal side), and double cluster (DC), in both full-length-VWF and in a VWF construct spanning D′ to A3 domains. Mutations did not alter VWF secretion by HEK293T cells, multimeric structure, or static collagen binding. The T1255A, Clus1, and DC variants caused increased ristocetin-mediated GPIbα binding to VWF. Platelet translocation rate on OLG mutants was increased because of reduced numbers of GPIbα binding sites but without effect on bond lifetime. In contrast, OLG mutants mediated increased platelet capture on collagen under high shear stress that was associated with increased adhesion of these variants to the collagen under flow. These findings suggest that removal of OLGs increases the flexibility of the hinge linker region between the D3 and A1 domain, facilitating VWF unfolding by shear stress, thereby enhancing its ability to bind collagen and capture platelets. These data demonstrate an important functional role of VWF OLGs under shear stress conditions. (*Blood*. 2012;120(1):214-222)

Introduction

von Willebrand factor (VWF) plays a critical role in facilitating primary hemostasis by supporting platelet adhesion and aggregation at sites of vascular injury.[1,2] VWF is synthesized and stored in endothelial cells and megakaryocytes and is released into the plasma as a series of multimers, with the largest being the most hemostatically active.[3]

After vascular injury, globular VWF binds to the exposed subendothelium, principally collagen, that in concert with conditions of shear stress, enables VWF to assume an extended conformation, resulting in exposure of its A1 domains, allowing them to interact with platelet receptor glycoprotein (GP) Ibα. This transient binding initiates platelet capture, a crucial step in a sequence of signaling and adhesion events that leads to formation of primary platelet plug.

The GPIbα-A1 bond lifetime is determined by the degree of shear applied, with flow enhancing the interaction similarly to the interaction between leukocyte selectins and sialyl Lewis^x–containing ligands.[4] Initially, as force increases, bond lifetime increases and cell rolling velocity decreases until a maximal value is reached (catch regime). As the force increases further, bond lifetimes decrease and platelet rolling velocities consequently increase (slip regime).[4]

Pro-VWF undergoes co- and posttranslational modifications, including addition of 16 *N*- and 10 *O*-linked glycans (OLGs) that comprise 18.7% of the total molecular weight.[5,6] *O*-linked glycosylation is initiated by α-*O*-linking of *N*-acetylgalactosamine to the β-hydroxyl group of either a serine or a threonine of the polypeptide chain and takes place in Golgi apparatus.[7] After addition of the first residue, OLGs are synthesized by sequential addition of monosaccharides by specific transferases to produce various "core" structures that can be extended by addition of further sugars such as sialic acid or modified by sulfation or acetylation. Although there is no consensus sequence, the likelihood of *O*-glycosylation can be predicted from comparative studies, based on the amino acid sequence surrounding the Ser/Thr residue. OLGs perform a variety of functions. First, they can block the accessibility of the peptide backbone to proteases and thus alter the plasma half-life of proteins.[8-11] Second, they mediate intracellular trafficking and are ligands for cell surface receptors; for example, they modulate leukocyte adhesion and rolling at sites of inflammation and on the endothelial surface.[12,13] Finally, *O*-linked oligosaccharides influence the structure of the protein by introducing steric hindrance to folding and confer a more rigid, extended conformation to the peptide backbone.[14,15]

VWF *N*-linked glycans have been studied extensively, although the data on the role of VWF OLGs are limited and often contradictory.[16,17] VWF lacking *O*-glycans is synthesized, multimerized, secreted, and binds heparin and collagen type I in the same way as the fully glycosylated form.[18] We recently published a detailed study of the VWF *O*-glycome composition showing the presence of unusual disialosyl motifs and ABH-bearing core 2 structures.[19] However, the ability of VWF deficient in OLGs to interact with platelets has not been fully explored. VWF lacking OLGs exhibited diminished reactivity with GPIb and ristocetin-induced platelet agglutination but exhibited normal platelet binding potential in the presence of botrocetin.[18] Conversely, isolated VWF-A1 domain devoid of OLGs exhibited increased platelet aggregation potential.[20] There are also limited data regarding the

Submitted February 9, 2012; accepted April 12, 2012. Prepublished online as *Blood* First Edition paper, April 19, 2012; DOI 10.1182/blood-2012-02-410050.

The online version of this article contains a data supplement.

The publication costs of this article were defrayed in part by page charge payment. Therefore, and solely to indicate this fact, this article is hereby marked "advertisement" in accordance with 18 USC section 1734.

correlation between VWF levels and its *O*-glycome. Recombinant VWF devoid of OLGs displayed a reduced half-life when administered in rats,[21] and an inverse correlation has been observed between VWF plasma levels and the presence of the most abundant VWF *O*-glycan, the sialylated core 1 structure.[22] The OLGs are positioned near the regions designated as important for platelet binding, suggesting they might be part of the mechanism regulating the exposure of the GPIbα binding site. Specifically, the *O*-glycan clusters might stabilize the potentially flexible linker regions flanking the A1 domain and thus modulate its interactions with vicinal domains. The aim of this study was to elucidate the role of the *O*-linked glycome and specific OLG residues in mediating VFW interaction with platelets.

Methods

VWF constructs and expression

Ten single VWF OLG variants—T1248A, T1255A, T1256A, S1263A, T1468A, T1477A, S1486A, T1487A, T1679A, and T2298A—and 3 cluster OLG variants—cluster 1 and cluster 2, lacking all 4 glycans flanking the N-terminal and C-terminal side of the A1 domain, respectively; and a double cluster [DC] variant lacking all glycans around the A1 domain—were generated in either full-length (FL)–VWF or VWF-D′A3 using the QuikChange XL site-directed mutagenesis kit (Stratagene). Details of vector construction and protein expression and purification can be found in supplemental Methods (available on the *Blood* Web site; see the Supplemental Materials link at the top of the online article). VWF ELISA, multimer analysis, and collagen and heparin binding were all performed as described previously.[16,23-25]

Binding to recombinant GPIbα binding under static conditions

Binding of VWF to recombinant GPIbα (rGPIbα) was performed essentially as described previously.[26] In brief; microtiter plates were coated with an anti-GPIbα (anti-CD42b) antibody (Santa Cruz Biotechnology) that has been shown not to inhibit GPIbα binding to the VWF A1 domain, at a final concentration of 5 μg/mL in 50mM carbonate buffer, pH 9.6, overnight at 4°C. After washing with phosphate-buffered saline supplemented with 0.1% Tween (PBS-T), wells were blocked with PBS/2.5% BSA and incubated with 1 μg/mL rGPIbα for 60 minutes at room temperature. The wells were washed with PBS-T and incubated with 1 μg/mL FL-VWF in the presence or absence of ristocetin (Helena Labs) for 1 hour. After washing, bound VWF was detected with horseradish peroxidase (HRP)–conjugated rabbit polyclonal anti-VWF antibodies (Dako United Kingdom) and color fast OPD substrate (Sigma-Aldrich).

Flow assays

All flow assays were performed using $VI^{0.1}$ flow slides (Ibidi) coated with either VWF or its variants or human type III collagen (Southern Biotechnology Associates). Washed platelets and erythrocytes were prepared essentially as described previously (supplemental Methods) and were perfused through the channels of the flow slide using a syringe pump (Aladdin-1000; World Precision Instruments) set to pump at defined flow rates giving a corresponding shear rate according to manufacturer's specifications. Flow slides were mounted on an epifluorescent microscope (CKX41; Olympus), and real-time recordings were captured via a Rollera XR camera (QImaging) and StreamPix6 4 software. Video images were analyzed offline using freely available Virtual Dub (http://www.virtualdub.org/) and MacBiophotonics ImageJ software (National Institutes of Health).

Measurement of platelet attachment and rolling velocity

Ibidi flow slides were coated with purified VWF-D′A3 and its variants at a final concentration of 30 μg/mL in carbonate buffer, pH 9.6, for 1 hour at room temperature. The flow channels were washed with PBS and blocked for 30 minutes with PBS-BSA. Reconstituted blood with a final platelet count of 140 000 cells/μL was then perfused through the channels at 400 to 2000 s^{-1}, and real-time videos (10 seconds) were captured after 4 minutes at 20 frames per second. The number of platelets after 4 minutes that remained stationary for 0.15 seconds was determined using ImageJ. Platelet translocation velocity was calculated by tracking individual platelets frame-by-frame using the ImageJ plug-in MtrackJ. The time that 1 platelet spent continuously moving (over a distance larger than the platelet diameter) while maintaining contact with the VWF-coated surface was defined as the rolling duration, and the rolling velocity was calculated by ImageJ from the distance that the platelet translocated during this period. For each VWF-D′A3 variant, 25 to 40 platelets were tracked in 3 fields of view for at least 3 separate experimental runs. To ensure that there was equal coating of all D′A3-VWF fragments onto the flow slides, immobilized proteins were recovered by filling the slide channels with stripping buffer (10mM Tris, 1mM EDTA, 2% SDS, 8M urea, and 0.01% bromphenol blue, pH 8.0) and incubating for 20 minutes at 60°C. The solution was aspirated from the channels and resolved using SDS-PAGE under reducing conditions, followed by Western blot and immunostaining with HRP-conjugated polyclonal anti-VWF antibody (Dako United Kingdom) or monoclonal mouse anti–c-myc (Santa Cruz Biotechnology) followed by secondary goat anti–mouse HRP (Dako United Kingdom).

Analysis of individual platelet tethering events under flow

The transient tether time between individual platelets and VWF-D′A3 molecules was determined essentially as described previously.[27,28] Ibidi slides were coated with 2 μg/mL VWF-D′A3 and reconstituted blood with a final platelet count of 140 000 cells/μL perfused through the channels at 400 to 2000 s^{-1}. A transient tether was defined as a flowing platelet that suddenly arrested, without translocation and then resumed a velocity equivalent to that of a noninteracting platelet. Only platelets that paused but did not roll were measured, and only 1 tethering event per platelet (in the field of view) was counted during the observation period. The duration of tethers was determined by recording images at a rate of 22 frames per second and measuring the time each platelet remained bound to the surface at a given shear rate. The dissociation rate constants were then determined by plotting the natural logarithm of the number of platelets that interacted as function of duration of tethering.[27,29,30] For first-order dissociation kinetics, the resultant plot is a straight line, and the slope of the line $= -k_{off}$. On average, 150 tethering events were measured to determine k_{off} in each independent experimental run. In addition, the number of transient tethering events over 5 seconds was calculated for each variant at 3 random fields of view.

VWF-mediated platelet capture on collagen

Ibidi flow slides were coated with 100 μg/mL human type III collagen overnight at 4°C and then washed and blocked as described in "Flow assays." Reconstituted blood was supplemented with 10 μg/mL recombinant FL-VWF or its variants and perfused through the flow channels at 1500 s^{-1} for 5 minutes. Short real-time videos were captured every 60 seconds, and the number of platelets captured, expressed as the percentage of the collagen surface that was covered, was determined using ImageJ. VWF adhesion to collagen was probed by perfusing FL-VWF in HEPES-Tyrode buffer, pH 7.4, supplemented with 1.5% BSA and 7% Ficoll at 1500 s^{-1} for 5 minutes. Flow through was collected, and the amount of unbound VWF measured by ELISA proteins bound to collagen were subsequently recovered by filling the slide channels with stripping buffer and incubating for 20 minutes at 60°C. The solution was then aspirated from the channels and resolved using SDS-PAGE under reducing conditions, followed by Western blot and immunostaining with HRP-conjugated polyclonal anti-VWF antibody (Dako United Kingdom). The density of bands (of size corresponding to VWF) was compared using MacBiophotonics ImageJ software.

Statistical analysis

Data analysis was performed using the Prism Software for Science software package (Version 4.0; GraphPad Software). Results are expressed as means ± SEM. The statistical significance of differences between 2 groups was assessed using Student *t* test. Differences between more than 2 groups were

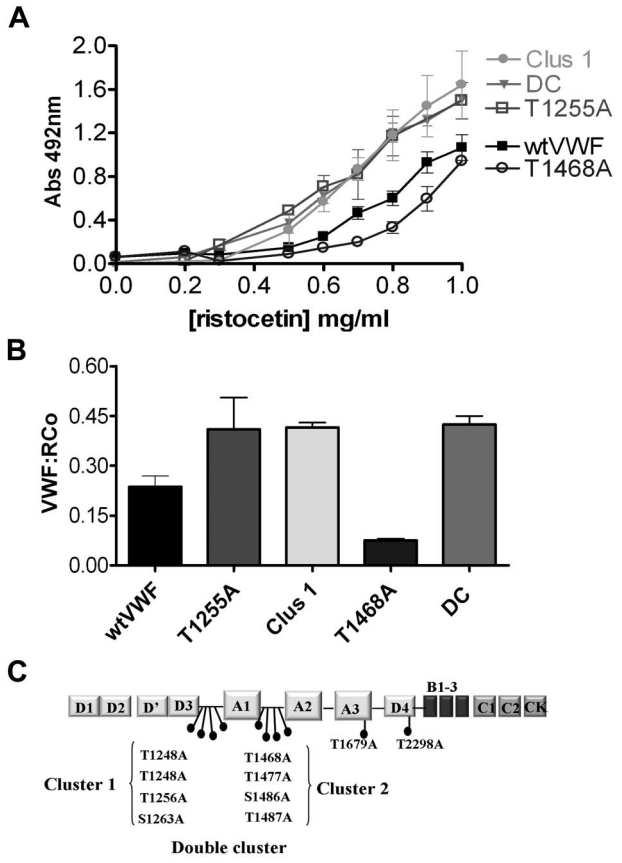

Figure 1. Binding of VWF *O*-glycosylation variants to recombinant GPIbα and platelets in the presence of ristocetin. (A) Binding of wt and OLG VWF variants to immobilized GPIbα in presence of increasing ristocetin concentrations. A GPIbα-coated plate was incubated with 4nM wtVWF or VWF variants in the presence of increasing ristocetin concentrations (0-1 mg/mL), and bound VWF was detected with polyclonal anti–VWF-HRP antibodies. Results were analyzed by ANOVA followed by Dunnett posttest. At 1 mg/mL, no significant difference in binding to GPIbα between wtVWF and OLG variants was observed. At all concentrations of ristocetin between 0.5 and 0.9 mg/mL, bindings were significantly different for wtWF and the T1255A, Clus1, and DC variants, with *P* values less than .03. (B) Ristocetin cofactor activity (VWF:RCo) of wt and OLG VWF variants measured by platelet agglutination with 1 mg/mL ristocetin ($P = .02$). Results are mean ± SEM of minimum 3 independent experiments performed in duplicate. (C) Schematic illustration of VWF monomer with positions of *O*-linked glycosylation sites indicated, and mutants generated.

evaluated using ANOVA and a Dunnett test for multiple comparison as well as Bonferroni adjustment. Statistical significance was set at $P < .05$.

Results

O-linked glycosylation of VWF does not influence expression, multimeric structure, or collagen binding

To investigate the functional role of VWF OLGs, we created a series of point mutations to prevent glycosylation at the 10 sites demonstrated by Titani et al[5] to be *O*-glycosylated. In addition, we generated 3 cluster variants to prevent *O*-linked glycosylation on either or both sides of the A1 domain (Figure 1C). All these variants were expressed and secreted at similar levels to wild-type (wt)VWF from HEK293T cells and demonstrated a similar multimeric structure to recombinant wtVWF (supplemental Figure 1). Furthermore, all the OLG variants had normal binding to collagen type I and III and heparin under static conditions (supplemental Figures 2-3). Finally, mass spectroscopy analysis of recombinant wtVWF showed that the *O*-linked glycome of VWF derived from HEK293T cells contained a similar range of structures to plasma-derived VWF (supplemental Figure 4; Table 1).

N-terminal OLG cluster modulates VWF interaction with GPIbα under static conditions

Previous studies have suggested that the OLGs flanking the A1 domain can influence the interaction with GPIbα; however, these data have often been conflicting and performed on isolated domains. We first assessed the binding of the OLG variants to rGPIbα in a plate-based ELISA assay in the presence of increasing ristocetin concentrations. No binding of wtVWF or any of the OLG variants was detected in the absence of ristocetin, demonstrating that removal of the OLG chains does not promote spontaneous GPIbα binding. In the presence of ristocetin, binding of wtVWF to GPIbα was evident at 0.6 mg/mL ristocetin and increased with increasing ristocetin concentration (Figure 1A). Interestingly, the T1255A, Clus1, and DC variants showed greater GPIba binding compared with wt at all ristocetin concentrations between 0.5 and 0.9 mg/mL ($P < .05$), indicating that the OLG located N-terminal to the A1 domain normally impair GPIbα binding, at least when induced by ristocetin. Conversely, the T1468A mutant showed slightly reduced binding to GPIbα at ristocetin concentration of 0.7 to 0.9 mg/mL. Similar results were obtained using the ristocetin cofactor assay (Figure 1B). For all other OLG variants, the binding pattern was indistinguishable from wtVWF (data not shown).

VWF OLGs modulate platelet translocation over VWF

To further investigate the modulation of VWF interaction with GPIbα by OLGs, we determined the ability of the VWF OLG mutants that had altered GPIbα binding in the static assay to capture platelets and mediate platelet translocation under shear. Flow slides were saturated with VWF-D′A3 or its variants, and the numbers of platelets captured and their rolling velocity measured at a range of shear rates. The D′A3 fragment was chosen because it does not form multimers; therefore, it can be used for kinetic studies in which spatial separation of the A1 domains is essential, while still encompassing the OLGs and structural elements that have been suggested to influence accessibility of the A1 domain.[31,32] We first confirmed that all the D′A3 mutants bound to the flow slides to a similar extent as wtD′A3. Immobilized proteins were recovered from the slides and analyzed by SDS-PAGE followed by Western blotting and immunostaining with both polyclonal anti-VWF antibody (Figure 2C) and anti–c-myc tag antibodies (Figure 2D). Densitometric analysis of bands corresponding to wtD′A3 and mutated D′A3 (115kDa) confirmed that all proteins used in the study were immobilized onto the slides with the same efficiency (Figure 2E; $P = .6$).

Table 1. Dissociation rate values for the tether bond between GPIbα receptor and wild type or mutated D′A3

	k_{off}			
Shear rate, s^{-1}	400	600	1000	2000
wtD′A3	6.7 ± 1.3	7.1 ± 1.1	7.1 ± 1.4	9.2 ± 1.6
DC-D′A3	5.4 ± 0.9	4.7 ± 0.6	5.7 ± 0.9	3.7 ± 0.4
T1255A-D′A3	6.6 ± .0.1	6.6 ± 0.8	6 ± 0.2	7.4 ± 1.7
Clus1-D′A3	5.5 ± 1.0	6.4 ± 1.2	5.1 ± 0.5	7.5 ± 1.6
T1468A	5.9 ± 0.9	6.9 ± 0.8	6.9 ± 0.9	7.9 ± 1.5

k_{off} values were calculated based on the duration of transient tethers at shear rates between 400 and 2000 $seconds^{-1}$. Values are mean ± SEM of 3 separate experiments. Results were analyzed by ANOVA followed by Bonferroni adjustment for multiple comparisons.

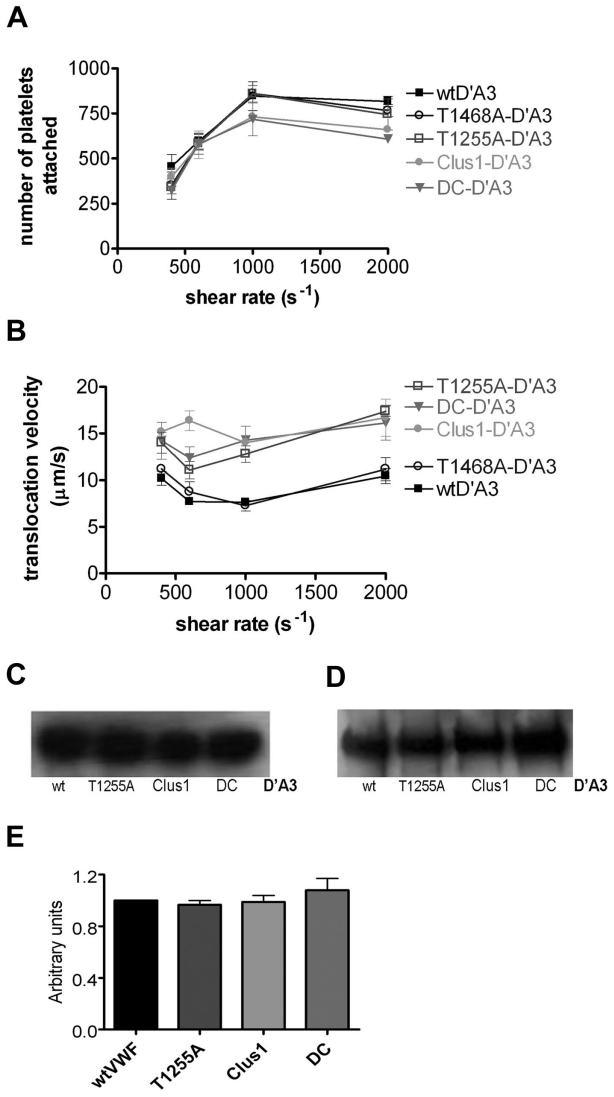

Figure 2. Comparison of platelets attachment and translocation velocities on immobilized VWF-D′A3 under shear stress. Fluorescently labeled platelets were perfused over immobilized wtD′A3 or its variants at shear rates from 400 to 2000 s^{-1} for 4 minutes. (A) After 4 minutes, the number of platelets that remained stationery for the duration of 3 frames (0.15 seconds) on the indicated substrates as a function of shear rate determined using ImageJ. (B) Translocation velocities ($\mu m/s^{-1}$) were measured by tracking individual platelets frame by frame at an interval of 0.05 second, in the direction of flow (n = 30 platelets for each 3 fields of view). Values shown are mean ± SEM of at least 4 independent experiments performed in duplicate. (C-D) To ensure equal D′A3 VWF coating, wtD′A3 OLG variants were immobilized onto flow slides. Next, after perfusion of PBS through the slides at 1000 s^{-1}, the bound protein was recovered from the channels using 2× SDS-PAGE reducing buffer and heating for 30 minutes, and then analyzed by SDS-PAGE followed by Western blotting with polyclonal anti–VWF-HRP–conjugated antibodies (C) or anti–c-myc antibodies (D). (E) Intensity of the bands (corresponding to VWF, ~ 260 kDa) was determined using MacBiophotonics ImageJ software and expressed as a proportion of wtD′A3 ($P = .6$).

Similar numbers of platelets were captured by either wt or mutant FL-VWF or D′A3 at all shear rates tested (data not shown). Platelets were captured by VWF in a shear-dependent manner and translocated along the surface in the direction of flow. The wtD′A3, T1255A-, Clus1-, and DC-D′A3 variants captured a similar increasing number of platelets from 400 to 1000 s^{-1}, which then fell slightly between 1000 and 2000 s^{-1} (Figure 2A). Furthermore, the T1468A variant that demonstrated reduced GPIbα binding under static conditions captured similar numbers of platelets to wtD′A3 at all the shear rates tested. (Figure 2A), and so did other mutants (data not shown). The differences in platelet capture were only statistically significant for Clus1 ($P = .02$) and DC ($P = .016$) at 2000 s^{-1}. Next, we analyzed platelet translocation velocity over the VWF variants between 400 and 2000 s^{-1} (Figure 2B). In keeping with previous studies, platelet translocation varied in a broadly biphasic manner, with the rolling velocity decreasing between 400 and 1000 s^{-1} before increasing again up to 2000 s^{-1}. The T1468A-D′A3 mutant demonstrated similar rolling velocities to wtD′A3 at all shear rates tested, indicating that this mutation does not affect GPIb binding under flow conditions. Significantly, although platelets translocated across the T1255A, Clus1, and DC-D′A3 variants in a broadly biphasic manner, the rolling velocity at each shear was increased compared with wtD′A3 (Figure 2B). All other mutants were able to support platelets rolling at the same velocity as wtD′A3 (data not shown).

VWF OLGs do not affect the duration of the GPIbα-VWF A1 bond but affect the number of bonds formed

Because platelets were observed to translocate faster across the T1255A, Clus1, and DC-D′A3 variants, we hypothesized that this may be because of either reduction in the duration of the VWF A1-GPIbα bond or an increase in the distance between each VWF binding point in the rolling path. To examine individual VWF-platelet bond lifetimes, we coated flow slides with a low concentration of D′A3-VWF that could mediate transient tethering but not translocation. The dissociation rate (k_{off}) was calculated as described previously by plotting the natural log of the number of tethering events against the duration of the tether (Figure 3A).[27-29] No significant difference was seen between the k_{off} values obtained for wtD′A3 and the *O*LG variants ($P = > .05$) at all the shear rates tested (DC at 2000 s^{-1}; $P = .03$ but not significant after Bonferroni correction for multiple comparisons), suggesting that the N-terminal OLGs do not affect bond duration (Table 1). Interestingly, we noted that with the T1255A, Clus1, and DC-D′A3 variants fewer tethering events took place over the duration of the assay. We therefore determined the number of transient tethering events that occurred over a set time period across a range of shear stress. The formation of transient tethers on wtD′A3 was inversely correlated with shear stress, with the maximal number of tethers formed at 400 s^{-1} (Figure 3B). Interestingly, the number of transient tethers formed on the T1255A, Clus1, and DC variants was greatly decreased at all shear rates, with the T1255A and Clus1 variants only able to tether minimal numbers of platelets. The DC variant was able to support marginally more tethering events at all shear rates compared with the T1255A and Clus1 variants (Figure 3B).

N-terminal *O*-glycans determine the A1 domain availability for GPIb binding

Although slides saturated with the T1255A, Clus1, and DC variants were able to capture similar numbers of platelets as wtD′A3 when the flow slides were coated at a low (2 μg/mL) concentration, many fewer platelet tethering events were observed on the variants compared with wtD′-A3. To investigate this further, we coated flow slides with increasing concentrations of VWF-D′A3 and analyzed platelet movement over these surfaces. At a coating concentration of 2 μg/mL, transient tether formation was the only type of interaction observed on either wtD′A3 or T1255A-, Clus1, or DC-D′A3, with significantly more tethers seen on wtD′A3. At 3, 7, and 15 μg/mL, more platelets interacted with wtD′A3, and a transition from transient tethers to rolling events was observed (Figure 4). In contrast, although T1255A-, Clus1-, and DC-D′A3

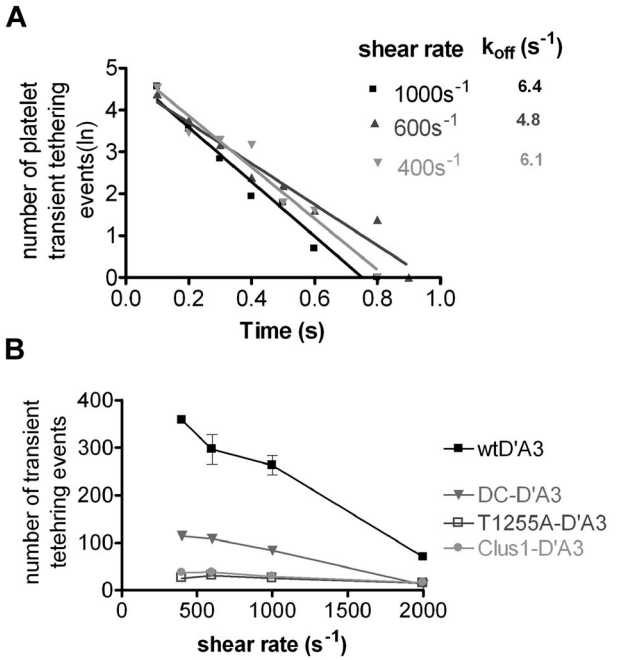

Figure 3. Kinetics of GPIbα-A1 interaction. (A) Disassociation rate constants were estimated at wall shear stresses between 400 and 2000 s^{-1} using a 2 μg/mL coating concentration of recombinant protein based on the duration of transient tether events. Kinetics of transient tethering between platelets and DC-D′A3 variant at a shear rates of 400, 600, and 1000 s^{-1} is demonstrated as an example. The natural logarithm of the number of tethering events (~ 150 individual interactions) was plotted against the duration of tethering and the negative slope of the lines is the k_{off}. Disassociation rate values at each shear rate are indicated (R^2 values were ~ 0.9). (B) Rate of platelet tethering to either wtD-A3 or OLG variants was plotted a function of shear rate. The graph shows the number of platelets that transiently tethered to each substrate at a given shear rate, during 5 seconds at 3 different fields of view (0.4 × 0.3 mm). Values are shown as mean ± SEM of 3 independent experiments.

also supported a greater number of tethering events as the concentration increased from 3 to 15 μg/mL, it remained lower than for wtD′A3, and it was only at 30 μg/mL that OLG variants were able to support platelet rolling and capture to the same extent as wtD′A3 (Figure 4). Thus, at subsaturating conditions, loss of the glycans at T1255, the entire N-terminal glycan cluster or all 8 OLGs flanking the A1domain reduces the ability of surface-bound VWF to interact with platelets. In light of this observation, we hypothesized that when directly coated to the flow slide surface the VWF OLG variants adopt a conformation such that a smaller proportion of A1-GPIb sites are available for platelet binding. Therefore, platelets translocate faster because although the bond lifetime is unchanged, the distance between available binding sites is greater. To assess this, we performed a detailed analysis of platelet translocation over wtD′A3 and the OLG variants. By taking Z-projections of 35 individual frames the pattern of platelet translocation could be observed (Figure 5). Interestingly, individual platelets movement across wtD′A3 seemed relatively smooth with minimal "gaps" in the translocation, whereas platelet movement across the T1255A, Clus1 and DC variants was less uniform with gaps present in the Z-projection so that platelets were observed to "jump" (Figure 5). These data suggest that when translocating over the mutant VWF surface, the distance between available A1 domains is increased and the resulting translocation velocity of platelets is increased.

T1255A, Clus1, and DC VWF *O*-glycan variants enhance VWF mediated platelet capture to collagen under flow

We next analyzed the ability of the OLG variants to mediate platelet capture to collagen under shear stress. Reconstituted blood was supplemented with recombinant VWF, perfused over collagen-coated slides at 1500 s^{-1}, and platelet capture was recorded in real time. As expected, in the absence of VWF, minimal platelet binding was observed, but with the addition of wtVWF the amount of bound platelets increased with time (Figure 6A). Significantly, platelet capture was enhanced to a greater extent when the T1255A, Clus1, or DC variants were added to reconstituted blood (Figure 6A). This may reflect either enhanced binding of platelets to these variants or an increased ability of these variants to bind to collagen under flow conditions. To investigate the latter hypothesis, VWF was diluted to a final concentration of 10 μg/mL in HEPES-Tyrode buffer and perfused over collagen-coated flow slides in the absence of platelets or erythrocytes. The bound protein was stripped from the flow slide and analyzed by Western blotting. Increased amounts of the T1255A, Clus1, and DC variants were recovered from the collagen surface compared with wtVWF (Figure 6B-C), suggesting that increased binding to collagen or self-association under flow conditions is at least in part, the explanation for enhanced platelet capture observed with these OLG variants. Because the OLG mutants did not affect collagen binding under static conditions, collagen-coated flow slides were incubated with wtVWF or mutant VWF under static conditions before the perfusion of plasma-free blood. Under these conditions, similar numbers of platelets were

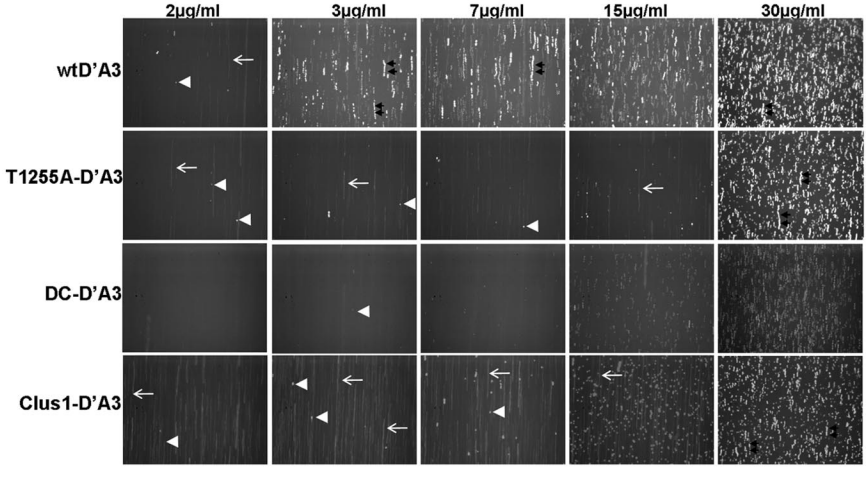

Figure 4. Interaction of platelets with increasing concentrations of wtD′A3 T1255-, Clus1, and DC-D′A3. Flow slides were coated with wtD′A3 and T1255A, Clus1 and DC-D′A3 at concentrations from 2 to 30 μg/mL, and labeled platelets were perfused at 1500 s^{-1} for 4 minutes. Videos were recorded in real time at a rate of 20 frames per second and 35 frames were superimposed using the high-intensity Z-projection function in ImageJ to visualize the nature of interaction between platelet and VWF. Representative images are shown. Examples of transient tethering events are indicated with white arrowheads, and platelet rolling is indicated with double black arrows. Platelets flowing near the surface, but not interacting, are visible as a white smears (white long arrow).

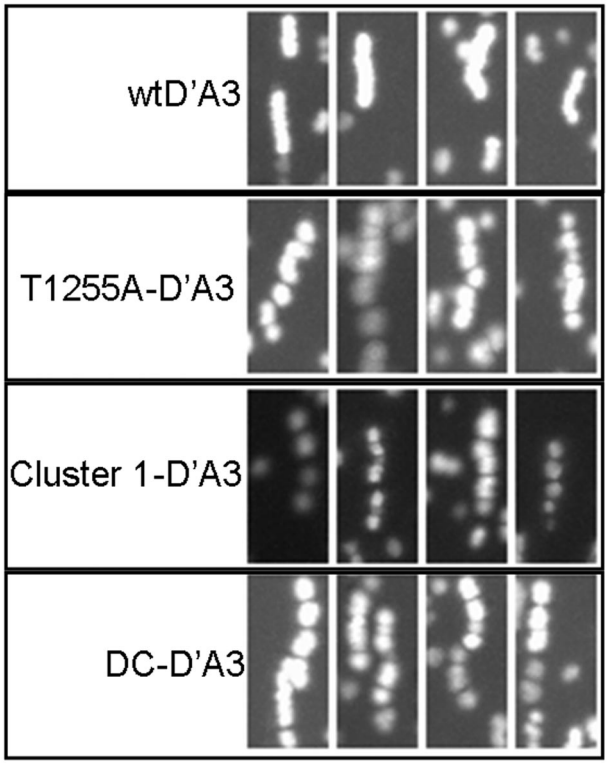

Figure 5. Platelet translocation pattern on immobilized wtD′A3 and T1255-, Clus1-, and DC-D′A3 glycosylation variants. Purified platelets were perfused over slides with D′A3 fragments immobilized at a concentration of 30 μg/mL at shear rate of 1000 s^{-1} for 4 minutes. Thirty-five subsequent frames were superimposed (~ 1.75 seconds) to track the translocation of individual platelets. Examples of platelets translocation paths on wt and mutated proteins are shown. When platelets jump rather than roll larger gaps between points of binding are seen; whereas when platelet roll uniformly and bind frequently no gaps are observed. Images were acquired at ×20 magnification and analyzed following ×3 zoom using ImageJ.

able to bind to collagen slides coated with wtVWF and T1255A-, Clus1-, and DC-VWF ($P = .62$; Figure 6D). These results indicate that loss of these OLGs increases the ability of VWF to bind to collagen under shear stress.

Discussion

The existing data regarding the function of VWF OLGs, especially their role in mediating VWF–platelet interactions, are conflicting and inconclusive; therefore, in the present study, we have investigated their role in the interaction of VWF with GPIbα and platelets under static and flow conditions. All the recombinant VWF OLG variants generated were expressed normally. The multimeric pattern and collagen and heparin binding activity of the mutants were similar to that of recombinant wtVWF, although they all show a reduction in high-molecular-weight multimers compared with plasma VWF. Thus, a specific contribution from mutations in high-molecular-weight cannot be excluded by these comparisons. The analysis of VWF binding to recombinant GPIbα under static conditions demonstrated that the T1255A, Clus1, and DC variants had significantly increased sensitivity to ristocetin-mediated GPIbα binding. Similar results were obtained using the ristocetin cofactor assay, and together these data suggest that the OLGs clustered on the N-terminal side of the A1 domain have an inhibitory effect on GPIbα binding, at least in the presence of ristocetin. In contrast, the T1468A variant showed slightly decreased GPIbα binding and platelet aggregation. This result is in keeping with previous observations in which membrane expressed VWF-A1 domain with the same mutation demonstrated reduced ristocetin-induced platelet agglutination.[20] However, under flow conditions, in the absence of ristocetin, this mutation did not affect platelet capture. The likeliest explanation for this result is that the reduced GPIbα binding observed in the static assay arises from destabilization of the ristocetin binding site encompassing the glycosylated T1468 residue.[33]

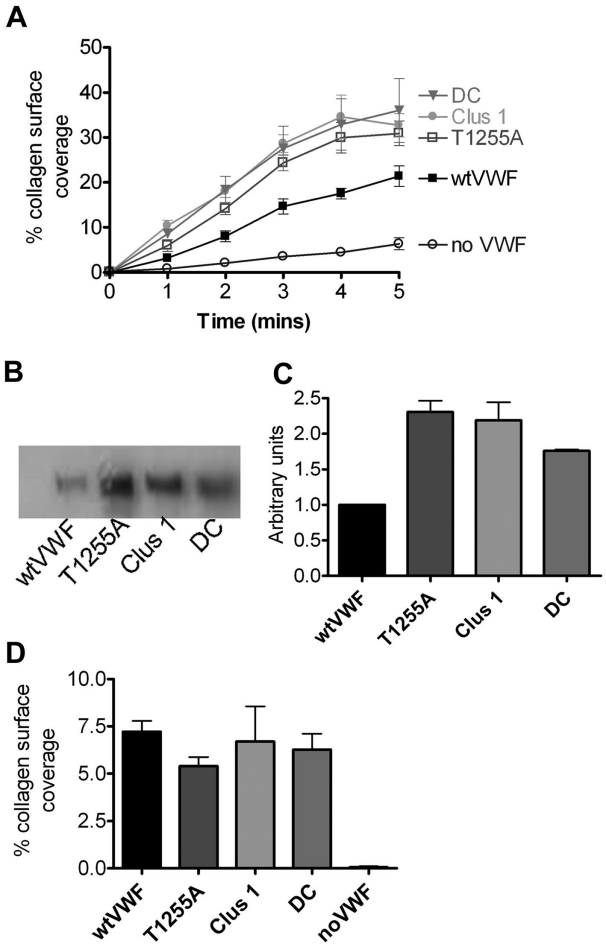

Figure 6. Platelet adhesion to collagen type III in the presence of wtVWF and VWF glycosylation variants under high shear stress. (A) Platelets resuspended in plasma-free blood supplemented with 10 μg/mL wtVWF or VWF OLG variants were perfused over a collagen type III–coated surface at 1500 s^{-1} for 5 minutes. Videos were processed off-line, and platelets that remained attached over the duration of 3 subsequent frames (0.15 seconds) were counted. The number of bound platelets is expressed as the percentage of surface coverage and is plotted against time after the start of perfusion. To ensure the specificity of the interaction, platelets without VWF were used. Values shown are mean ± SEM of minimum 3 independent experiments performed in duplicate. (B) wtVWF and VWF variants were perfused over collagen type III–coated surface at a shear rate of 1500 s^{-1} for 5 minutes. Bound proteins were recovered from the slides using 2× SDS-PAGE reducing buffer and heating at 60°C for 30 minutes and then analyzed by SDS-PAGE followed by Western blotting with polyclonal anti–VWF-HRP–conjugated antibodies. (C) Intensity of the bands corresponding to VWF (~ 260 kDa) was determined using ImageJ and expressed as a proportion of wtVWF (mean ± SEM of 3 independent experiments). (D) wtVWF and OLG variants at a concentration of 10 μg/mL were bound under static conditions to flow slides coated with collagen type III. Next, platelets resuspended in plasma-free blood were perfused over at 1500 s^{-1} for 5 minutes, and videos were processed off-line as described in panel A. The number of bound platelets is expressed as the percentage of surface coverage after the 5 minutes from initiation of perfusion. Values shown are mean ± SEM of minimum 3 independent experiments. One-way ANOVA was used to determine differences, and the *P* value was calculated to be .62.

To analyze the effect of the OLG variants under more physiologic conditions, in vitro flow assays were used. Platelets bound to wtD′A3 or the OLG variants in a generally similar, shear-dependent manner. In accordance with previously published studies, platelet rolling velocities on all constructs were dependent on the shear rate, with a biphasic velocity curve. Interestingly, platelets translocated almost 2-fold faster on the T1255A-, Clus1-, and DC-D′A3 variants than on the wt protein. To gain insight into the kinetics of transient tether events between platelets and VWF, the flow slides were coated at low protein concentration as described previously to limit multiple bond formation and to allow for assessment of individual platelet-VWF binding events.[27,34] The dissociation rate constants of transient tethers to wtD′A3 were of the same order of magnitude as reported, although previous studies used isolated bacterial A1 domains at lower shear rates.[27,35,36] Interestingly, no significant difference in the dissociation rate constants for bonds formed between platelets and OLG mutants were detected compared with wtD′A3. This excludes an effect of OLG on VWF-platelet dissociation as an explanation for the increased translocation rates. However, when coated at low concentration it was apparent that the T1255A-, Clus1-, and DC-D′A3 variants supported notably lower numbers of transient tethering events compared with wtD′A3 between 400 and 1000 s^{-1}. Because we have shown that all variants are equally and efficiently immobilized onto the slides, this finding implies that a proportion of immobilized D′A3 variants cannot form bonds, presumably because of reduced accessibility of GPIbα binding sites in the absence of OLGs flanking the A1 domain. This effect on platelet recruitment is not observed when slides are saturated with protein, because individual platelets can interact with more than 1 A1 domain, thus allowing adhesion, even if a proportion of the GPIbα binding sites are not available. Subsequently, we demonstrated that T1255A, Clus1, and DC-D′A3 had to be immobilized at concentrations 10 times higher than wtD′A3 to support platelet rolling. We therefore propose that when the OLG variants are immobilized onto a surface the distance between available A1 domains is increased. Consequently, under flow, platelets pause less frequently and cover a greater distance over a given time period, which is reflected in a faster platelet translocation velocity. The dependence of rolling velocity on the density of potential interaction sites has been demonstrated previously by Fredrickson et al in a study using mammalian cells expressing GPIbα and immobilized VWF.[37]

Next, we used the flow assay to evaluate VWF-mediated platelet capture to collagen. Intriguingly, the FL-VWF variants, T1255A, Clus1, and DC were shown to mediate increased platelet capture to collagen under flow. By perfusing these mutants over a collagen surface in the absence of platelets and then stripping the bound VWF from the surface, we demonstrated that increased amounts of the VWF OLG variants were bound under shear stress, either because they bind more readily to collagen in these conditions or possibly because self-association of VWF molecules was increased. This would account, in part, for the increased platelet capture observed. Interestingly, we have shown that when VWF is bound under static conditions to collagen, and plasma-free blood is perfused over at high shear stress similar platelet capture is observed for wtVWF and OLG variants. Because OLG mutants adhered normally to collagen under static conditions, we conclude that removal of OLGs enhances unravelling and subsequent collagen binding under shear stress, rather than directly altering platelet binding. In this circumstance, the A1 domain seems to be readily available for platelet binding, whereas when directly immobilized on a surface, VWF devoid of OLGs seems to be captured in a more tightly folded conformation, with the accessibility of the GPIbα binding sites being limited. Both instances may reflect a reduction in stiffness of the D3-A1 linking peptide in the absence of OLG. This effect also may facilitate the alteration of VWF conformation by ristocetin, explaining the observed increase in GPIb binding.

Previous work on OLGs has shown that they introduce steric hindrance and provide rigidity to peptide backbones; they can extend and stabilize otherwise flexible regions, thus stabilizing protein conformations.[14,38-40] It has been shown than on a hydrophobic surface VWF adopts a coiled structure, thought to resemble VWF in solution.[41] We conclude that removal of the OLG(s) adjacent to the A1 domain increases flexibility of the linker regions, allowing VWF to adopt a more tightly folded conformation, and thereby increasing interaction of the A1 domain with vicinal domains and limiting exposure of GPIbα binding site. Immobilization on a hydrophobic surface does not seem to alter this configuration and the A1 remains hidden. Conversely, for VWF in solution exposed to shear stress, increased flexibility of the hinge linker region between the D3 and A1 domains could make VWF lacking OLG(s) able to more completely unfold, enhancing its ability to bind collagen. The isolated A1 domain is able to bind to collagen and platelets, but in FL-VWF it is the interaction of the A3 domain with collagen that is essential to mediate platelet capture. VWF binding via A3 domains induces a conformational change in VWF, exposing its cryptic A1 collagen binding site.[42,43] It is possible that under shear stress and A3 binding to collagen, the absence of OLG(s) facilitates A1 exposure for collagen binding as well as platelet capture. Importantly, platelet adhesion to collagen under high shear stress depends on the presence of both soluble and collagen bound VWF to form a VWF network, which anchors circulating platelets.[44,45] It is also possible that the absence of OLG(s) enhances the ability of VWF to self-associate under conditions of high shear stress; however, this is unlikely because it has recently been shown that the A domains are not directly involved in VWF lateral self-association.[46]

Intriguingly, an individual glycan chain at T1255 has an impact on the interaction with GPIb comparable with the removal of entire glycan cluster, whereas other single mutants have none. This might imply that the observed effect on VWF function results from the loss of a single *O*-linked carbohydrate rather than cumulative response to the loss of several glycans. It has been shown previously that *O*-glycosylation occurs in a highly ordered and hierarchical manner and *N*-acetylgalactosaminyltransferases can have highly restricted acceptor substrates. Blocking glycosylation at T1255A might influence subsequent glycosylation events by inducing conformational changes in the peptide backbone and altering the accessibility of particular glycosylation sites for *N*-acetylgalactosaminyltransferases.[47-49] However, to date it has not been possible to ascertain whether mutation of a given OLG site of VWF affects glycosylation of nearby residues.

Together, the presented data support the hypothesis that OLG(s) present in the hinge, linker region connecting the D3-A1 domains, modulates VWF-platelet interaction both in the presence of ristocetin and shear stress. Importantly, however, the effect of the OLGs seems to be mediated by altering accessibility of the A1 domain in these conditions rather than by an effect on VWF A1-GPIbα bond. This is particularly evident under shear and when different forms of immobilization are used. Moreover, OLGs influence VWF ability to adhere to collagen, self-associate, or both in the presence of hydrodynamic shear stress. In view of the presented data, it is clear that GPIb binding to VWF is a complex event and that distinct

structural characteristics can control the ability to establish stable bonds or to initiate platelet tethering. These results also emphasize the importance of the immobilization method when studying VWF receptor–ligand interactions under shear. Comparison of the results obtained on plastic slides with those obtained on collagen exemplifies this problem.

Acknowledgments

This work was supported by grants from the British Heart Foundation (RG/06/007 and FS/06/064/21 490) and by an Amersham funded studentship (A.A.N.).

Authorship

Contribution: A.A.N. and T.A.J.M. designed the study, performed experiments, analyzed results, and wrote the manuscript; K.C. performed experiments and analyzed results; A.R. performed experiments; and M.A.L. designed the study and wrote the manuscript.

Conflict-of-interest disclosure: The authors declare no competing financial interests.

Correspondence: Thomas A. J. McKinnon, Department of Haematology, Imperial College London, 5th Floor, Commonwealth Building, Hammersmith Hospital Campus, Du Cane Rd, London W12 0NN, United Kingdom; e-mail: t.mckinnon03@imperial.ac.uk.

References

1. Sadler JE. Biochemistry and genetics of von Willebrand factor. *Annu Rev Biochem.* 1998;67:395-424.
2. Federici AB. The factor VIII/von Willebrand factor complex: basic and clinical issues. *Haematologica.* 2003;88(6):EREP02.
3. Wagner DD. Cell biology of von Willebrand factor. *Annu Rev Cell Biol.* 1990;6:217-246.
4. Marshall BT, Long M, Piper JW, Yago T, McEver RP, Zhu C. Direct observation of catch bonds involving cell-adhesion molecules. *Nature.* 2003;423(6936):190-193.
5. Titani K, Kumar S, Takio K, et al. Amino acid sequence of human von Willebrand factor. *Biochemistry.* 1986;25(11):3171-3184.
6. Samor B, Mazurier C, Goudemand M, Debeire P, Fournet B, Montreuil J. Preliminary results on the carbohydrate moiety of factor VIII/von Willebrand factor (FVIII/vWf). *Thromb Res.* 1982;25(1-2):81-89.
7. Hanisch FG. O-glycosylation of the mucin type. *Biol Chem.* 2001;382(2):143-149.
8. Garner B, Merry AH, Royle L, Harvey DJ, Rudd PM, Thillet J. Structural elucidation of the N- and O-glycans of human apolipoprotein(a): role of o-glycans in conferring protease resistance. *J Biol Chem.* 2001;276(25):22200-22208.
9. Smith KA. Interleukin-2: inception, impact, and implications. *Science.* 1988;240(4856):1169-1176.
10. Altschuler Y, Kinlough CL, Poland PA, et al. Clathrin-mediated endocytosis of MUC1 is modulated by its glycosylation state. *Mol Biol Cell.* 2000;11(3):819-831.
11. Hang HC, Bertozzi CR. The chemistry and biology of mucin-type O-linked glycosylation. *Bioorg Med Chem.* 2005;13(17):5021-5034.
12. Ley K, Kansas GS. Selectins in T-cell recruitment to non-lymphoid tissues and sites of inflammation. *Nat Rev Immunol.* 2004;4(5):325-335.
13. Hermiston ML, Xu Z, Weiss A. CD45: a critical regulator of signaling thresholds in immune cells. *Annu Rev Immunol.* 2003;21:107-137.
14. Jentoft N. Why are proteins O-glycosylated? *Trends Biochem Sci.* 1990;15(8):291-294.
15. Shogren R, Gerken TA, Jentoft N. Role of glycosylation on the conformation and chain dimensions of O-linked glycoproteins: light-scattering studies of ovine submaxillary mucin. *Biochemistry.* 1989;28(13):5525-5536.
16. McKinnon TA, Chion AC, Millington AJ, Lane DA, Laffan MA. N-linked glycosylation of VWF modulates its interaction with ADAMTS13. *Blood.* 2008;111(6):3042-3049.
17. McKinnon TA, Goode EC, Birdsey GM, et al. Specific N-linked glycosylation sites modulate synthesis and secretion of von Willebrand factor. *Blood.* 2010;116(4):640-648.
18. Carew JA, Quinn SM, Stoddart JH, Lynch DC. O-linked carbohydrate of recombinant von Willebrand factor influences ristocetin-induced binding to platelet glycoprotein 1b. *J Clin Invest.* 1992;90(6):2258-2267.
19. Canis K, McKinnon TA, Nowak A, et al. The plasma von Willebrand factor O-glycome comprises a surprising variety of structures including ABH antigens and disialosyl motifs. *J Thromb Haemost.* 2010;8(1):137-145.
20. Schulte am Esch J, 2nd Robson SC, Knoefel WT, Eisenberger CF, Peiper M, Rogiers X. Impact of O-linked glycosylation of the VWF-A1-domain flanking regions on platelet interaction. *Br J Haematol.* 2005;128(1):82-90.
21. Stoddart JH Jr, Andersen J, Lynch DC. Clearance of normal and type 2A von Willebrand factor in the rat. *Blood.* 1996;88(5):1692-1699.
22. van Schooten CJ, Denis CV, Lisman T, et al. Variations in glycosylation of von Willebrand factor with O-linked sialylated T antigen are associated with its plasma levels. *Blood.* 2007;109(6):2430-2437.
23. Favaloro EJ. Collagen binding assay for von Willebrand factor (VWF:CBA): detection of von Willebrands disease (VWD), and discrimination of VWD subtypes, depends on collagen source. *Thromb Haemost.* 2000;83(1):127-135.
24. Baillod P, Affolter B, Kurt GH, Pflugshaupt R. Multimeric analysis of von Willebrand factor by vertical sodium dodecyl sulphate agarose gel electrophoresis, vacuum blotting technology and sensitive visualization by alkaline phosphatase anti-alkaline phosphatase complex. *Thromb Res.* 1992;66(6):745-755.
25. O'Donnell J, Boulton FE, Manning RA, Laffan MA. Amount of H antigen expressed on circulating von Willebrand factor is modified by ABO blood group genotype and is a major determinant of plasma von Willebrand factor antigen levels. *Arterioscler Thromb Vasc Biol.* 2002;22(2):335-341.
26. Vanhoorelbeke K, Cauwenberghs N, Vauterin S, Schlammadinger A, Mazurier C, Deckmyn H. A reliable and reproducible ELISA method to measure ristocetin cofactor activity of von Willebrand factor. *Thromb Haemost.* 2000;83(1):107-113.
27. Doggett TA, Girdhar G, Lawshe A, et al. Selectin-like kinetics and biomechanics promote rapid platelet adhesion in flow: the GPIb(alpha)-vWF tether bond. *Biophys J.* 2002;83(1):194-205.
28. Alon R, Chen S, Puri KD, Finger EB, Springer TA. The kinetics of L-selectin tethers and the mechanics of selectin-mediated rolling. *J Cell Biol.* 1997;138(5):1169-1180.
29. Ramachandran V, Yago T, Epperson TK, et al. Dimerization of a selectin and its ligand stabilizes cell rolling and enhances tether strength in shear flow. *Proc Natl Acad Sci U S A.* 2001;98(18):10166-10171.
30. Alon R, Hammer DA, Springer TA. Lifetime of the P-selectin-carbohydrate bond and its response to tensile force in hydrodynamic flow. *Nature.* 1995;374(6522):539-542.
31. Ulrichts H, Udvardy M, Lenting PJ, et al. Shielding of the A1 domain by the D′D3 domains of von Willebrand factor modulates its interaction with platelet glycoprotein Ib-IX-V. *J Biol Chem.* 2006;281(8):4699-4707.
32. Martin C, Morales LD, Cruz MA. Purified A2 domain of von Willebrand factor binds to the active conformation of von Willebrand factor and blocks the interaction with platelet glycoprotein Ibalpha. *J Thromb Haemost.* 2007;5(7):1363-1370.
33. De Luca M, Facey DA, Favaloro EJ, et al. Structure and function of the von Willebrand factor A1 domain: analysis with monoclonal antibodies reveals distinct binding sites involved in recognition of the platelet membrane glycoprotein Ib-IX-V complex and ristocetin-dependent activation. *Blood.* 2000;95(1):164-172.
34. Ramachandran V, Nollert MU, Qiu H, et al. Tyrosine replacement in P-selectin glycoprotein ligand-1 affects distinct kinetic and mechanical properties of bonds with P- and L-selectin. *Proc Natl Acad Sci U S A.* 1999;96(24):13771-13776.
35. Doggett TA, Girdhar G, Lawshe A, et al. Alterations in the intrinsic properties of the GPIbalpha-VWF tether bond define the kinetics of the platelet-type von Willebrand disease mutation, Gly233Val. *Blood.* 2003;102(1):152-160.
36. Kumar RA, Dong JF, Thaggard JA, Cruz MA, Lopez JA, McIntire LV. Kinetics of GPIbalpha-vWF-A1 tether bond under flow: effect of GPIbalpha mutations on the association and dissociation rates. *Biophys J.* 2003;85(6):4099-4109.
37. Fredrickson BJ, Dong JF, McIntire LV, Lopez JA. Shear-dependent rolling on von Willebrand factor of mammalian cells expressing the platelet glycoprotein Ib-IX-V complex. *Blood.* 1998;92(10):3684-3693.
38. Naganagowda GA, Gururaja TL, Satyanarayana J, Levine MJ. NMR analysis of human salivary mucin (MUC7) derived O-linked model glycopeptides: comparison of structural features and carbohydrate-peptide interactions. *J Pept Res.* 1999;54(4):290-310.
39. Cyster JG, Shotton DM, Williams AF. The dimensions of the T lymphocyte glycoprotein leukosialin and identification of linear protein epitopes that can be modified by glycosylation. *EMBO J.* 1991;10(4):893-902.
40. McMaster TJ, Berry M, Corfield AP, Miles MJ. Atomic force microscopy of the submolecular architecture of hydrated ocular mucins. *Biophys J.* 1999;77(1):533-541.
41. Raghavachari M, Tsai H, Kottke-Marchant K, Marchant RE. Surface dependent structures of von Willebrand factor observed by AFM under

aqueous conditions. *Colloids Surf B Biointerfaces.* 2000;19(4):315-324.

42. Morales LD, Martin C, Cruz MA. The interaction of von Willebrand factor-A1 domain with collagen: mutation G1324S (type 2M von Willebrand disease) impairs the conformational change in A1 domain induced by collagen. *J Thromb Haemost.* 2006;4(2):417-425.
43. Lankhof H, van Hoeij M, Schiphorst ME, et al. A3 domain is essential for interaction of von Willebrand factor with collagen type III. *Thromb Haemost.* 1996;75(6):950-958.
44. Savage B, Almus-Jacobs F, Ruggeri ZM. Specific synergy of multiple substrate-receptor interactions in platelet thrombus formation under flow. *Cell.* 1998;94(5):657-666.
45. Choi H, Aboulfatova K, Pownall HJ, Cook R, Dong JF. Shear-induced disulfide bond formation regulates adhesion activity of von Willebrand factor. *J Biol Chem.* 2007;282(49):35604-35611.
46. Ulrichts H, Vanhoorelbeke K, Girma JP, Lenting PJ, Vauterin S, Deckmyn H. The von Willebrand factor self-association is modulated by a multiple domain interaction. *J Thromb Haemost.* 2005;3(3):552-561.
47. Hanisch FG, Muller S, Hassan H, et al. Dynamic epigenetic regulation of initial O-glycosylation by UDP-N-acetylgalactosamine:peptide N-acetylgalactosaminyltransferases. site-specific glycosylation of MUC1 repeat peptide influences the substrate qualities at adjacent or distant Ser/Thr positions. *J Biol Chem.* 1999;274(15):9946-9954.
48. Kirnarsky L, Nomoto M, Ikematsu Y, et al. Structural analysis of peptide substrates for mucin-type O-glycosylation. *Biochemistry.* 1998;37(37):12811-12817.
49. Tetaert D, Ten Hagen KG, Richet C, Boersma A, Gagnon J, Degand P. Glycopeptide N-acetylgalactosaminyltransferase specificities for O-glycosylated sites on MUC5AC mucin motif peptides. *Biochem J.* 2001;357(Pt 1):313-320.